

Glycopeptides with Sialyl Lewis Antigen in Serum Haptoglobin as Candidate Biomarkers for Nonalcoholic Steatohepatitis Hepatocellular Carcinoma Using a Higher-Energy Collision-Induced Dissociation Parallel Reaction Monitoring–Mass Spectrometry Method

Yu Lin, Jianhui Zhu,* Jie Zhang, Jianliang Dai, Suyu Liu, Ana Arroyo, Marissa Rose, Amit G. Singal, Neehar D. Parikh, and David M. Lubman*



Cite This: *ACS Omega* 2022, 7, 22850–22860



Read Online

ACCESS |



Metrics & More

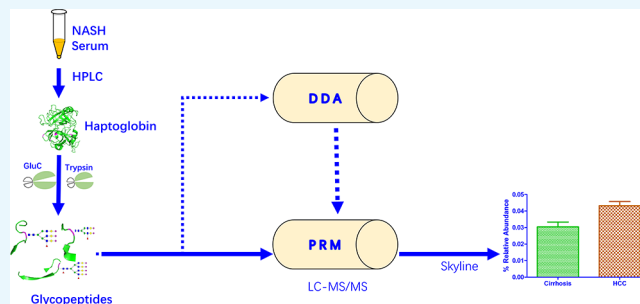


Article Recommendations



Supporting Information

ABSTRACT: Nonalcoholic steatohepatitis (NASH) is the fastest growing cause of hepatocellular carcinoma (HCC) in the United States. Changes in *N*-glycosylation on specific glycosites of serum proteins have been investigated as potential markers for the early detection of NASH-related HCC. Herein, we report a glycopeptide with a Sialyl Lewis structure derived from serum haptoglobin (Hp) as a potential marker for NASH related HCCs among 95 patients with NASH, including 46 cirrhosis, 32 early-stage HCC, and 17 late-stage HCC. Hp immuno-isolated from patient serum was analyzed using LC-HCD-PRM-MS/MS followed by data analysis *via* Skyline software. Two glycopeptides involving site N184 and four glycopeptides involving site N241 were significantly changed in patients with HCC *vs* NASH cirrhosis ($P < 0.05$). The two-marker panel using *N*-glycopeptide N241_A4G4F2S4 showed the best performance for HCC detection when combined with α -fetoprotein (AFP), with an improved estimated area under the curve (AUC) = 0.898 (95% CI: 0.835, 0.951), compared to the AUC of 0.790 (95% CI, 0.697–0.872) using AFP alone ($P = 0.048$). At 90% specificity, the combination of N241_A4G4F2S4 + AFP had an improved sensitivity of 63.3%, compared to the sensitivity of 52.3% using AFP alone. When using three markers, the panel of AFP + N241_A2G2F1S2 + N241_A4G4F2S4 yielded an estimated AUC of 0.928 (95% CI: 0.877, 0.970). Our findings indicated that N241_A4G4F2S4 may play an important role in distinguishing HCC from NASH cirrhosis.



INTRODUCTION

Nonalcoholic steatohepatitis (NASH) is one of the leading causes of chronic liver disease in the United States.^{1,2} NASH can lead to cirrhosis and subsequent hepatocellular carcinoma (HCC) at an incidence of 1–2% per year.³ Due to its poor survival rate at advanced stages, early stage detection of HCC is needed for effective clinical treatment.⁴ Ultrasound-based surveillance, the current standard of care, has poor sensitivity for early-stage HCC detection, particularly in patients with NASH-given issues of operator dependency and poor visualization.^{5,6}

Many serum proteins are secreted from the liver, where aberrant serum proteins could serve as potential molecular indicators of liver disease.^{7–10} Among these, alpha-fetoprotein (AFP) has been widely used for surveillance and HCC prognosis.¹¹ However, AFP has not been recommended by the American Association for the Study of Liver Diseases (AASLD) due to its poor sensitivity (approximately 60%) and specificity (80%) for early-stage HCC with a common cut-

off value of 20 ng/mL.¹² AFP-L3, a form of AFP, which has high affinity to *Lens culinaris agglutinin* (LCA) bearing a core-fucosylated glycoform at site N251, has been approved by the US Food and Drug Administration (FDA) for use as a serum biomarker for HCC diagnosis. However, AFP-L3 cannot overcome the limitation of low sensitivity compared to AFP with an overall sensitivity of AFP-L3 for HCC of approximately 50–60%.¹³ A biomarker with improved sensitivity and specificity for early-stage HCC diagnosis is required.

Recent studies have reported that glycosylation alterations of serum proteins may serve as a marker for the early diagnosis of

Received: April 26, 2022

Accepted: June 13, 2022

Published: June 22, 2022



cancer.^{7,10,14–17} Other studies have explored site-specific glycosylation structural changes in serum glycoproteins as potential markers for early HCC, including ceruloplasmin,¹⁸ kininogen-1,¹⁹ α -1-antitrypsin,²⁰ and vitronectin.⁷ Serum haptoglobin (Hp), containing four glycosites at N184, N207, N211, and N241, is an abundant glycoprotein secreted into the bloodstream primarily by the liver, where it modulates renal iron loading and prevents kidney damage by releasing iron.²¹ Hp also has been reported as a reporter protein based on aberrant glycosylation for several cancers.^{22–26}

Recent advances in mass spectrometry (MS) have provided powerful techniques for verification of site-specific glycopeptide markers to aid in early detection of cancer^{27–29} based on subtle but significant glycosylation changes in the same peptide.^{7,22} The fucosylated and sialylated glycan structures of serum Hp have been shown to be significantly elevated in patients with HCC compared to patients with cirrhosis.³⁰ In related work, glycan structural changes of Hp in liver related diseases, such as hepatitis B virus (HBV),³¹ hepatitis C virus (HCV),²⁴ and alcohol-related liver disease,³² have been observed using MS-based techniques.²³ In our previous work, we have mapped the landscape of site-specific glycosylation of serum Hp in patients with HCC and cirrhosis using LC-ETcD-MS/MS and demonstrated the potential for detecting subtle changes in site-specific N-glycopeptides for discrimination of early HCC from cirrhosis.^{22,23} However, a more specific and targeted study of glycan changes of these glycopeptides of Hp needs to be investigated.

In the current work, we have performed further biomarker discovery to select the optimal glycopeptide markers for discrimination of HCC from cirrhosis and early HCC from cirrhosis. We have thus used parallel reaction monitoring-tandem mass spectrometry combined with liquid chromatography (LC-PRM-MS/MS) to quantitatively evaluate the changes in targeted site-specific glycopeptides of serum Hp, as determined by potential marker candidates for detection of early NASH HCC from cirrhosis in our previous study,²² among 95 NASH-related patients, including 46 cirrhosis, 32 early-stage HCCs, and 17 late-stage HCCs. The quantitative analysis results were evaluated by receiver operating characteristic curves (ROC), where six glycopeptides demonstrated significant changes between NASH-related HCC and cirrhosis patients. A glycopeptide with Sialyl Lewis antigen among these six Hp glycopeptides, from the N241 site, was finally determined as an optimal biomarker for potential diagnosis of HCC in patients suffering from NASH cirrhosis for monitoring NASH disease progression.

MATERIALS AND METHODS

Reagents. Sequencing-grade trypsin and GluC were purchased from Promega (Madison, WI, USA). The 7KDa MWCO Zeba Spin Desalting Columns were purchased from Thermo Scientific (Rockford, IL, USA). Hp standard protein was purchased from Abcam. Other reagents were from Sigma (St. Louis, MO, USA).

Serum Samples. Serum samples from patients were provided by UT Southwestern Medical Center, Dallas, Texas, including NASH cirrhosis ($n = 46$), early-stage NASH HCC ($n = 32$), and late-stage NASH HCC ($n = 17$). Samples were aliquoted and stored at $-80\text{ }^{\circ}\text{C}$, without prior thaw cycles. Samples were approved by the IRB at UTSW and then transferred to the University of Michigan using a material transfer agreement between institutions. Other details are as

described in previous works.^{33–37} The clinical features are summarized in Table 1. These 95 serum samples were

Table 1. Clinical Characteristics of Individual Patients with NASH^a for Investigation^a

variable	cirrhosis	early HCC	late HCC	<i>p</i> -value
<i>N</i>	46	32	17	
gender (M/F)	13/33	15/17	11/6	0.026 [§]
age	61.5 [25, 84]	70.7 [60, 91]	64 [43, 78]	<0.001
laboratory				
AFP	3 [1.4, 10]	5 [2.0, 310.4]	101.9 [4, 60,500]	<0.001
total_bilirubin	0.7 [0.2, 4.1]	0.7 [0.2, 4.7]	1.6 [0.3, 3.1]	0.121
INR	1.1 [0.9, 2.6]	1.1 [0.9, 2.5]	1.1 [1.0, 1.9]	0.527
creatinine	0.94 [0.48, 7.4]	0.95 [0.59, 3.69]	0.83 [0.41, 7.47]	0.249
score				
MELD_score	8 [0, 24]	8.5 [1, 21]	8 [1, 30]	0.775
CTP score	6 [5, 10]	5 [1, 10]	6 [2, 11]	0.058
ascites (%)				
1. None	35 (76.1)	23 (71.9)	11 (64.7)	
2. Mild	9 (19.6)	9 (28.1)	5 (29.4)	
3. Severe	2 (4.3)	0 (0.0)	1 (5.9)	
TNM				
I	0	21	0	
II	0	11	0	
III	0	0	11	
IV	0	0	6	
AFP < 20 ng/mL	46 (100.0)	26 (81.2)	5 (29.4)	<0.001 [§]
max_diameter	NA [NA, NA]	3.05 [1.3, 12.0]	14.75 [8.5, 18.5]	<0.001

^aValues are presented as median with the range [min, max]. *p*-Values with “[§]” are obtained from Fisher’s exact test; all others are obtained from the Kruskal–Wallis Test. AFP, TBili, ALT, AST, INR, and creatinine values and MELD and CTP scores were provided by the UT Southwestern Medical Center. Values are presented as median with the interquartile range (IQR). AFP: alpha-fetoprotein; TBili: total bilirubin; ALT: alanine aminotransferase; AST: aspartate aminotransferase; INR: international normalized ratio; MELD: Model for end stage liver disease; CTP: Child–Turcotte–Pugh.

classified as two groups: 46 NASH cirrhosis and 49 NASH HCC (32 early-stage and 17 late-stage NASH HCC). Early-stage disease was defined by Milan criteria. The analysis was performed using R 4.0.5.

Haptoglobin Purification. The experimental process is shown in Figure 1. An in-house antibody-immobilized HPLC column was used to purify the Hp protein from 20 μL of each individual patient serum where the resulting sample was then digested and analyzed by MS. Details are included in our prior publications.²²

Double Enzymatic Digestion, Glycopeptide Enrichment. Double enzymatic digestion and glycopeptide enrichment were performed as described previously (see ref 22).

LC-Stepped HCD-DDA-MS/MS and LC-Stepped-HCD-PRM-MS/MS. To obtain the parameters of the targeted precursors such as the retention time, charges, and ratio of mass to charges, a survey scan in DDA mode was required before running the PRM analysis. The dried glycopeptides were dissolved in distilled water containing 0.1% formic acid (FA) and then analyzed on an Orbitrap Fusion Lumos Tribrid

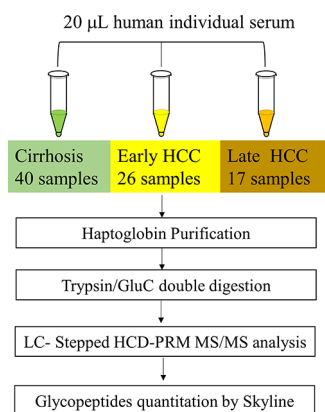


Figure 1. Workflow of the quantitative N-glycopeptide analysis.

mass spectrometer (Thermo) coupled with a Dionex UPLC system with conditions as described in our prior work.^{7,10,22} The mass spectrometer was set as data dependent mode with the MS1 scan range set as m/z 400–2000 and MS1 data acquired in the Orbitrap (120k resolution, $4e^5$ AGC, 100 ms injection time) followed by stepped HCD-MS/MS acquisition with the stepped collision energies of 31.5, 35, and 38.5%. When the LC-Stepped HCD-PRM-MS/MS was performed, the elution linear gradient was like that used in the DDA detection mode mentioned above. Two differences between DDA-MS/MS and PRM-MS/MS involving the stepped collision energies (19, 26, 33%) were set to fragment the glycopeptides, and the PRM analysis required pre-defined precursor ions. As a method of targeted quantitative analysis, the sensitivity of the detection of PRM is improved compared to the DDA detection mode. The targeted precursor ions from Hp are listed in Table S1, which include potential glycopeptide markers with mono- and bi-fucosylated glycans at sites N184, N207, and N241 and those with fully sialylated bi- and tri-antennary glycan motifs.

The MS proteomics data have been placed in the ProteomeXchange Consortium via the PRIDE partner repository (<http://www.ebi.ac.uk/pride/archive/>) with the dataset identifier PXD.

Method Reproducibility and Linear Dynamic Range.

LC stepped-HCD-PRM-MS/MS was employed to quantitatively target and analyze the glycopeptides where a standard Hp protein was digested to assess reproducibility. The double digestion procedure was the same as described above. For these reproducibility experiments, four repeated independent experiments were carried out where $1 \mu\text{g}$ of Hp-digested product was injected into the MS for each run. For linear regression analysis, different amounts (0.25, 0.5, 0.75, 1.0, 1.5, and $2 \mu\text{g}$) of digested product from Hp were injected sequentially, and the XIC from the results were plotted against the amount of the protein injected.

Data Interpretation and Relative Quantitation. All spectra from DDA results were searched with Byonic software (Protein Metrics), as described previously.⁷ A UniProt human Hp database (P00738) was used for data searching.^{23,25,38–40} The search parameters were set as in prior works.^{7,10} The theoretical m/z of the oxonium ions in glycopeptides from HCD-MS were used to check the fragment ions.^{7,22,23}

The Skyline platform was used to quantitatively analyze the selected glycopeptides from PRM results. Like DDA analysis, oxonium ions including HexNAc, NeuAc, HexNAc-Hex,

HexHexNAcFuc, and HexNAcHexNeuAc and other possible b/y ions, were used for glycopeptide identification, while the Y1 ion (peptide+HexNAc) was used for quantification.^{7,20} Skyline analysis requires peptide settings, transition settings, and a .ms2 file converted from the survey scan raw data. A fasta file (P00738 from UniProt human database) of haptoglobin was uploaded as the background protein database. Peptide settings are required to create a library (.ssl file) with the parameters taken from a DDA survey scan, such as the glycopeptide sequence, scan number, retention time, charges and so on. The transition settings and the procedures for quantification are as described in our recent publication.^{7,10}

RESULTS AND DISCUSSION

Patients' Characteristics. The patient serum samples classified as NASH cirrhosis and NASH HCC based on the clinical features are summarized in Table 1. Ninety-five patients were involved in this study, including 46 NASH cirrhosis, 32 NASH early-stage HCC, and 17 late-stage HCC. In respect to the laboratory tests, there was no statistically significant difference in total bilirubin, INR, and creatinine, whereas the AFP was statistically significant among these groups. In addition, there were no statistically significant differences in the MELD score and CTP score among these groups. These HCC patients involved different TNM stages, including 32 early-stage HCC (21 stage I and 11 stage II) and 17 late-stage HCC (11 stage III and 6 stage IV). The median age was 61.5 years old for NASH-related cirrhosis, 70.7 years old for NASH early-stage HCC, and 64.0 years old for late-stage HCC. It showed that the NASH-related HCC patients were more likely to be older patients than those with NASH-related cirrhosis ($P < 0.001$).

Statistical Method. Descriptive statistics were used to summarize the patient characteristics. The group difference was assessed using the Fisher's exact test for the discrete variables such as gender and using the Kruskal–Wallis test for continuous variables such as age. The marker distributions were summarized using the descriptive statistics such as the median and the range, as well as the histogram. The Wilcoxon test was used to compare their values between HCC and cirrhosis samples. The adjusted p -values using the Bonferroni correction for multiple comparisons were provided for each marker. The markers with clinical importance and showing statistically significant difference between HCC and cirrhosis were selected as the candidate markers for panel development. Their differentiation effect was evaluated using the area under the curve (AUC) based on the receiver operation characteristic (ROC) analysis. The logistic regression model was used to combine the site-specific glycopeptide biomarker candidates with AFP in the marker panel development. The best 2-marker and 3-marker panels were selected based on their estimated AUC. The bootstrapping method was used to compare the AUC of the selected panel to the AUC using AFP alone, i.e., test $H_1 : AUC_{\text{panel}} \neq AUC_{\text{AFP}}$ against $H_0 : AUC_{\text{panel}} = AUC_{\text{AFP}}$. A value of $P < 0.05$ was considered as statistically significant. All statistical analysis was performed using R Statistical Software (version 3.6.1; R Foundation for Statistical Computing, Vienna, Austria).

Method Reproducibility and Linear Dynamic Range.

Four repeated independent experiments were carried out using Hp standard protein then detected by LC-HCD-PRM-MS/MS. The Pearson correlation coefficient R^2 values for the binary comparison of the four technical replicates from 0.97 to

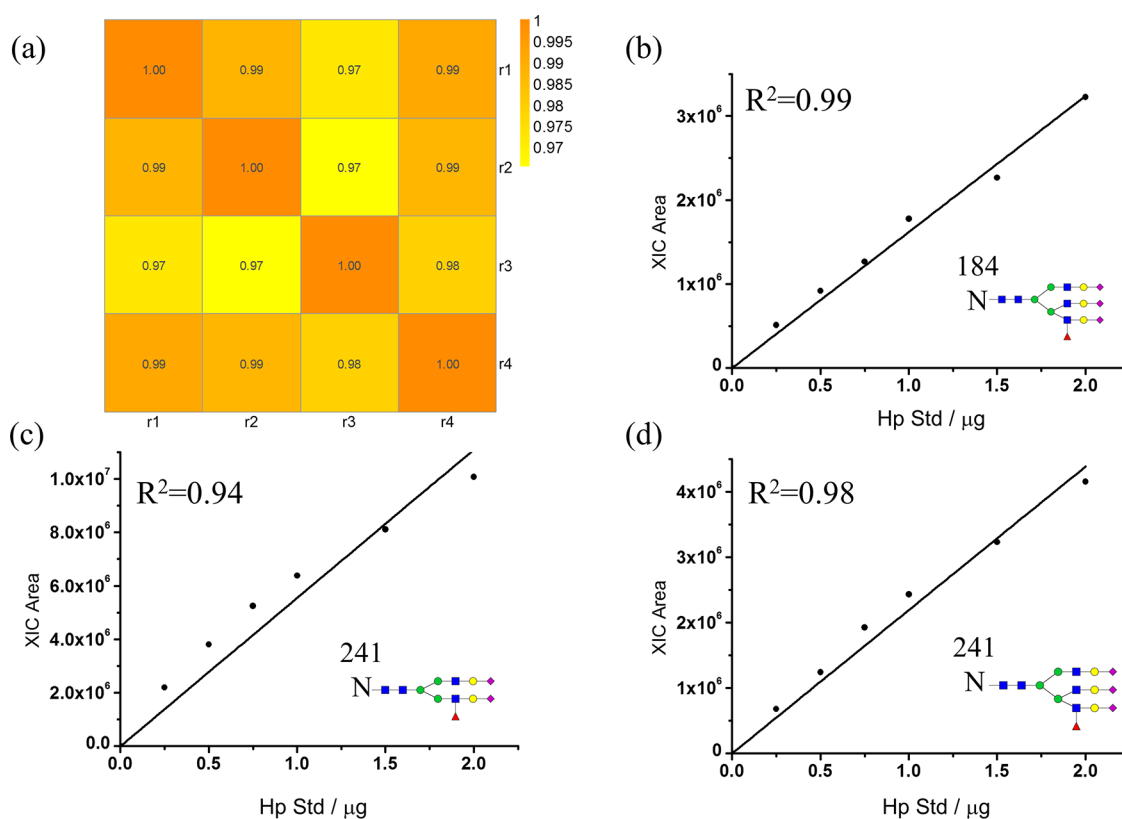


Figure 2. (a) Analysis of four independent replicates of the standard Hp sample. Pearson correlation coefficient R^2 values for the binary comparison of the three replicates ranging from 0.97 to 0.995. (b–d). Linear regression analysis of glycopeptides N184_A(3)G(3)F(1)S(3), N241_A(2)G(2)F(1)S(2), and N241_A(3)G(3)F(1)S(3) from the standard Hp sample, respectively.

0.99 as shown in Figure 2a indicated a good reproducibility for the experiment. Furthermore, the linear dynamic range of each glycopeptide was carried out by different amounts of Hp standard protein involving 0.25, 0.5, 0.75, 1.0, 1.5, and 2 μ g injection each time. The linear regression curves of these glycopeptides are shown in Figure 2b–d and Figure S1. The R^2 of these linear regression curves by the XIC against the amount of protein were between 0.94 and 0.99, indicating that all these glycopeptides have good reproducibility by this method when the injected proteins were in a range of 0.25–2 μ g. The results of linear regression analysis did not involve the tetra-antennary glycoform of glycopeptides since the level of these glycoform glycopeptides was extremely low in this Hp standard protein, which was derived from normal subjects.

Glycopeptides Identified as Potential Biomarker Candidates by LC-stepped-HCD-PRM-MS/MS. To confirm the differential expression of glycopeptides for diagnostic potential in the detection of NASH HCC, LC stepped-HCD-PRM-MS/MS was performed for targeted quantitative analysis of the selected glycopeptide candidates among different liver disease states, including 46 cirrhosis, 32 early-stage HCC, and 17 late-stage HCC.⁴¹ The selection of the targeted glycopeptides for PRM-MS was based on our previous report on the site-specific glycopeptides of Hp showing a significant difference during the progression from NASH cirrhosis to HCC by differential LC-DDA-MS/MS analysis.²² The glycopeptide marker candidates were predominantly found with fucosylated or fully sialylated glycan motifs. Although the overall fucosylation level of serum Hp in patients can be evaluated by a lectin-antibody enzyme-linked immunosorbent

assay (ELISA) method,⁴² the subtle but important changes of the glycoforms of Hp cannot be assessed by this method.

The significant advantage of PRM-MS is that it is a targeted quantitative analysis as compared to DDA-MS, which scans over the entire mass range. The increased sensitivity of PRM is due to its targeted nature where the mass spectrometer can spend longer times collecting the target peptide ions, which is termed dwell time, compared to DDA-MS. Also, PRM allows all fragment ions of a predefined precursor to be measured in parallel, where a full MS2 product ion spectrum of a specified precursor ion can be acquired, and all detectable product ions can be simultaneously monitored at high accuracy and resolving power.^{43,44} In addition, the PRM-MS can provide a wide dynamic range for quantitative analysis for target precursors.^{41,45} These aspects of PRM allow accurate quantification of a larger number of target precursors in an anticipated elution time interval.

In a recent work, it has been reported that four glycopeptides involving site N207 of Hp changes significantly in abundance between HCC and cirrhosis from a total of 30 patients' serum samples. It was further shown that when AFP was combined with glycopeptides N207_A3G3F1S2 and N207_A3G3F1S2 as a 3-marker panel, the result provided a better AUC value than AFP alone.⁴⁶ Different from this work, the current work contains a total of 95 patients' serum samples in a larger sample set and the precursor ions selected in our current experiment were based on our previous work^{22,23} where both charge states 3 and 4 precursor ions were included. These differences would provide more accurate and precise results, which include significant changes of glycopeptides in abundance involving sites N184 and N241.

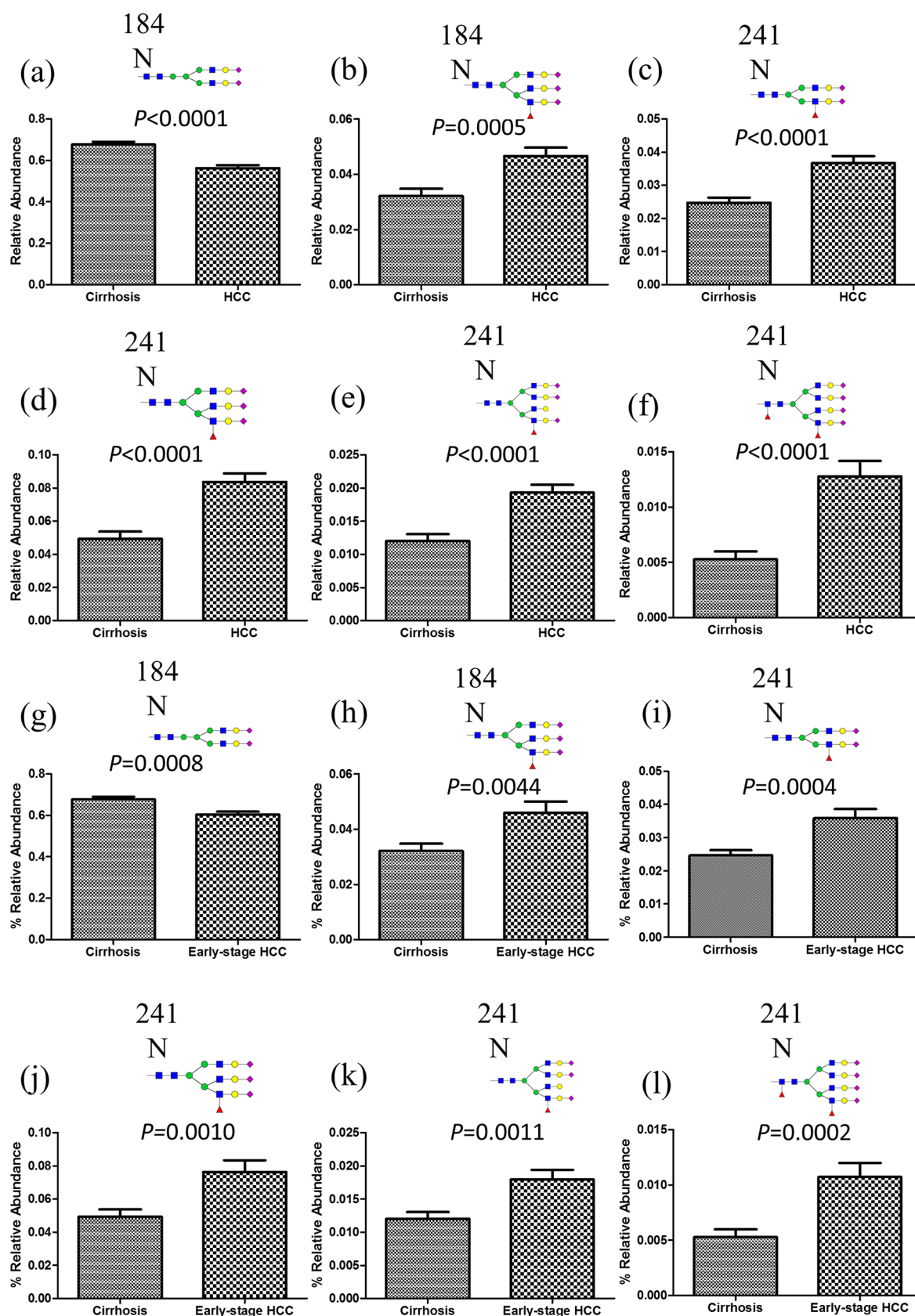


Figure 3. Histograms of the six differentially expressed site-specific *N*-glycopeptides between HCC and cirrhosis (a–f) as well as between early-stage HCC and cirrhosis (g–l).

In our current study, 49 precursor ions originating from 32 site-specific glycopeptides, including mono- and bi-fucosylated

glycoforms at sites N184, N207, and N241, were selected for PRM-MS analysis among different liver disease states (Table

Table 2a. Summary of the Six Candidate Glycopeptide Markers: Summary Statistics Using Median and Range, and Comparisons between All HCC and Cirrhosis^a

variable	median [min, max]		<i>P</i>	<i>P</i> _{adjusted}
	cirrhosis	all HCC		
<i>N</i>	46	49		
N184_A2G2S2	69.06 [50.51, 86.89]	57.88 [37.74, 76.36]	<0.001	<0.001
N184_A3G3F1S3	2.94 [0.33, 7.76]	4.96 [0.62, 10.11]	<0.001	0.008
N241_A2G2F1S2	2.36 [0.29, 5.54]	3.63 [0.93, 9.90]	<0.001	<0.001
N241_A3G3F1S3	4.40 [0.20, 16.81]	8.28 [2.52, 21.39]	<0.001	<0.001
N241_A4G4F1S3	1.16 [0.06, 3.18]	2.04 [0.16, 3.87]	<0.001	<0.001
N241_A4G4F2S4	0.46 [0.00, 2.13]	1.11 [0.19, 6.34]	<0.001	<0.001

^a*P* denotes the *p*-values based on the Wilcoxon test. *P*_{adjusted} denotes the adjusted *p*-values using Bonferroni correction, where *P*_{adjusted} = *P* × 32.

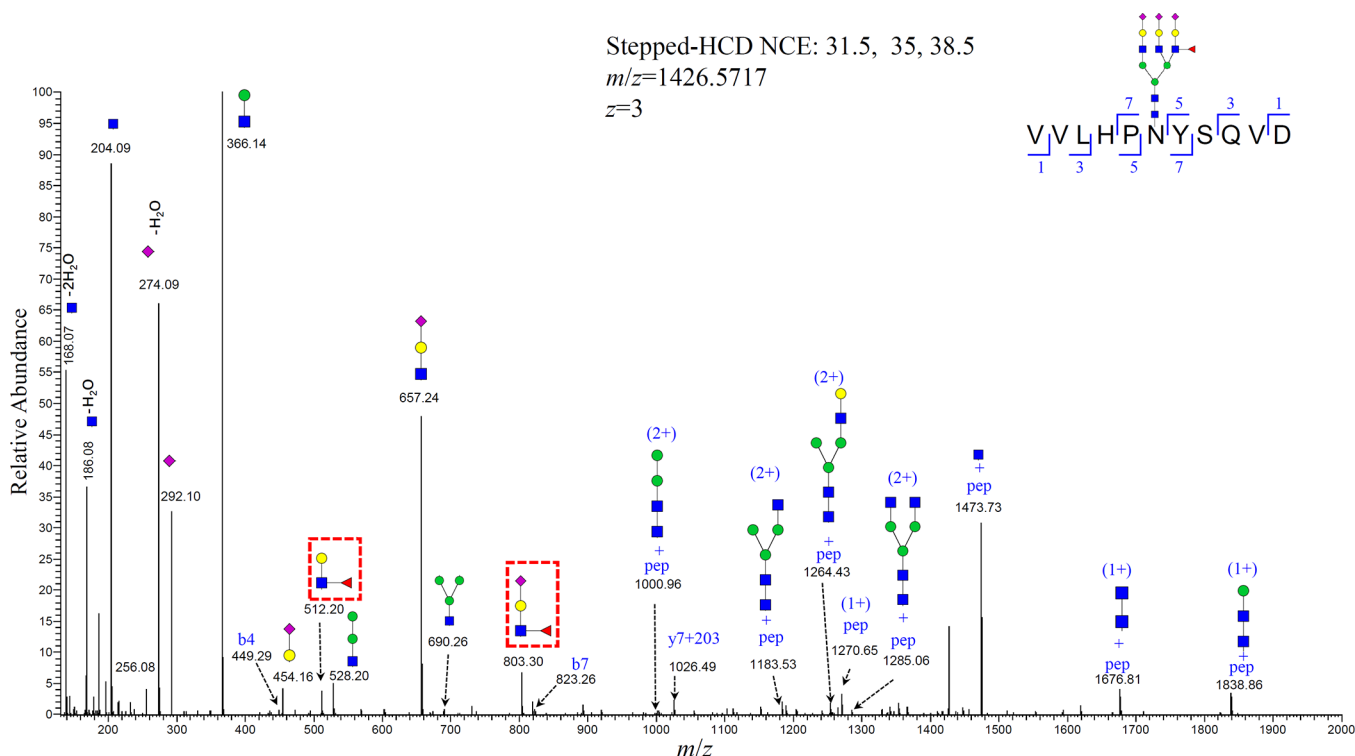


Figure 4. MS/MS spectrum of an *N*-glycopeptide N241_A3G3F1S3 (symbols used in the structural formulas: bluesquare = HexNAc; green circle = Man; yellow circle = Gal; red triangle = Fuc; purple diamond = NeuAc).

S1). Both charge states 3 and 4 of the precursor ion were included for PRM-MS in some glycopeptides based on the MS profile observed in the DDA mode. Based on the relative abundance of each glycopeptide quantified using the Skyline platform, the expression of six glycopeptides showed statistically significant differences between patients with HCC and those with cirrhosis (Figure 3). The relative abundance of each marker was normalized by their peak, and the normalized value was used for the ROC analysis. Table 2a summarizes their distribution using median and range, as well as the *p*-values based on the Wilcoxon test. After Bonferroni correction, their *p*-values were still statistically significant (<0.05). These six glycopeptides involved two glycosites—N184 and N241. The two glycopeptides on N184 were N184_A2G2S2 (Figure 3a) and N184_A3G3F1S3 (Figure 3b, mass spectrum in Figure S2). There are four glycopeptides derived from the same peptide backbone containing N241 including the bi-antennary glycoform N241_A2G2F1S2 (Figure 3c, mass spectrum in Figure S3), tri-antennary glycoform N241_A3G3F1S3 (Figure 3d, mass spectrum in Figure 4), tetra-antennary glycoform

N241_A4G4F1S3 (Figure 3e, mass spectrum in Figure S4), and N241_A4G4F2S4 (Figure 3f, mass spectrum in Figure 5). All four glycopeptides were increased significantly during the progression from cirrhosis to HCC. It is notable that the non-fucosylated glycopeptide N184_A2G2S2 was decreased during the progression of HCC, whereas the other five fucosylated glycan forms at sites N184 and N241 were elevated in HCC compared to cirrhosis, indicating the complexity of fucosylation and sialylation in HCC as previously reported.^{23,24,47} The expression of these six glycopeptides also presented statistically significant differences between patients with early-stage HCC and those with cirrhosis (Figure 3g–l).

It is important to point out that the oxonium ions at *m/z* 512.20 (HexNAc-Hex-Fuc) and *m/z* 803.30 (HexNAc-Hex-Fuc-NeuAc) were clearly observed in the mass spectra of these five fucosylated glycopeptides (Figures 4 and 5, Figures S2–S4), indicating that all of these fucosylated-bearing glycopeptides were outer-arm fucosylated. This is consistent with results reported from previous reports.²² Particularly, the fragment *m/z* 803.3 (HexNAc-Hex-Fuc-NeuAc) demonstrates that all these

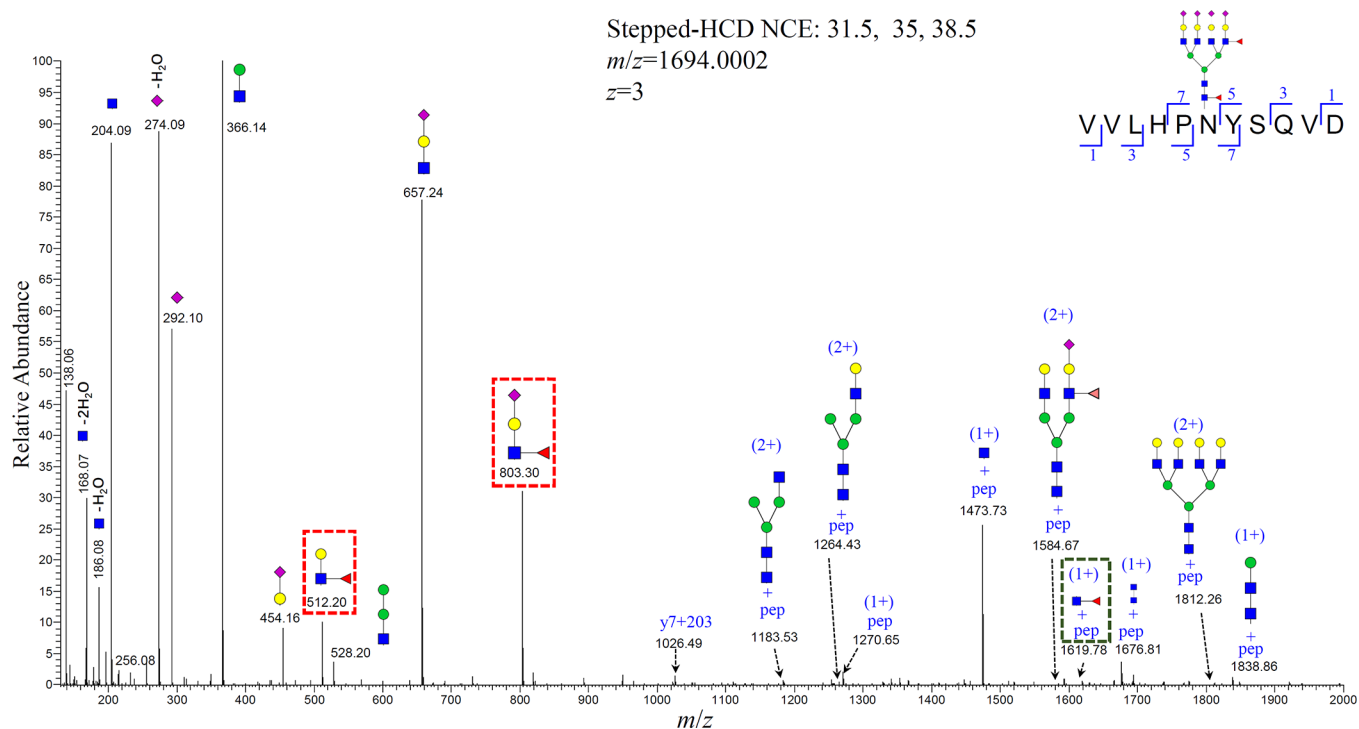


Figure 5. MS/MS spectrum of an *N*-glycopeptide of N241_A4G4F2S4 (symbols used in the structural formulas: bluesquare = HexNAc; green circle = Man; yellow circle = Gal; red triangle = Fuc; purple diamond = NeuAc).

Table 2b. Summary of the Six Candidate Glycopeptide Markers: Estimated AUC of Individual Markers for All HCCs and Early-Stage HCCs, Respectively

marker	cirrhosis ($n = 46$) vs all HCC ($n = 49$)			cirrhosis ($n = 46$) vs early HCC ($n = 32$)		
	AUC	95% CI	sensitivity at 90% specificity	AUC	95% CI	sensitivity at 90% specificity
AFP	0.790	(0.697, 0.872)	52.3%	0.715	(0.592, 0.827)	39.5%
N184_A2G2S2	0.776	(0.676, 0.866)	40.8%	0.703	(0.579, 0.819)	21.9%
N184_A3G3F1S3	0.719	(0.606, 0.820)	24.5%	0.682	(0.552, 0.806)	21.9%
N241_A2G2F1S2	0.765	(0.665, 0.853)	34.7%	0.732	(0.617, 0.832)	37.5%
N241_A3G3F1S3	0.796	(0.693, 0.883)	46.9%	0.729	(0.611, 0.836)	31.3%
N241_A4G4F1S3	0.758	(0.657, 0.853)	32.7%	0.704	(0.579, 0.818)	25.0%
N241_A4G4F2S4	0.793	(0.700, 0.874)	44.9%	0.757	(0.643, 0.861)	34.4%

glycopeptides bear Sialyl Lewis (SLe) antigen.⁴⁸ As the SLe antigens can be mainly classified as SLe^x and SLe^A, where their differences are the linkages between the fucosyl and HexNAc residues, which cannot be distinguished in mass spectrometry, we can consider them as SLe antigens together. The SLe^x epitopes in α -1-acid glycoprotein and haptoglobin from sera were found to have a different expression of SLe^x in small cell and non-small cell lung cancer patients.⁴⁹ Tang et al. employed SLe^A combined with CA19-9 as a potential diagnosis of pancreatic cancer.⁵⁰

Of interest, the mass spectrum of glycopeptide N241_A4G4F2S4, at m/z 1619.78 (pep + HexNAc+Fuc) presented a core-fucosylated glycoform (Figure 5). Combined with the fragments m/z 512.20 (HexNAc-Hex-Fuc) and SLe antigen (m/z 803.30, HexNAc-Hex-Fuc-NeuAc), this bi-fucosylated tetra-antennary glycopeptide at site N241 contained one outer-arm fucosylation as well as a core fucosylation. Saldova et al. combined SLe^x levels and core fucosylated agalactosylated diantennary glycan as complementary markers for CA125 in ovarian cancer diagnosis.⁵¹ We found that all the SLe epitope containing glycopeptides were increased significantly during the disease progression from

cirrhosis to late-stage HCC, whereas the N184_A2G2S2 decreased where this is a non-fucosylated glycopeptide.

Diagnostic Performance of Site-Specific *N*-Glycopeptides in All HCC and Early HCC. We performed the receiver operating characteristic (ROC) analysis for Hp site-specific *N*-glycopeptides in differentiating all HCCs and early HCCs from cirrhosis patients, respectively. The estimated AUC as well as its 95% confidence interval (CI) were summarized for each individual marker in Table 2b. AFP had an estimated AUC of 0.790 (95% CI: 0.697, 0.872), and the sensitivity was 52.3 at 90% specificity when comparing all HCC vs cirrhosis. The six glycopeptides derived from two glycosites N184 and N241 discussed above were all expressed statistically significantly different between cirrhosis and all HCC groups. The estimated AUCs of two glycopeptides involving the site N184 were 0.776 (95% CI: 0.676, 0.866) and 0.719 (95% CI: 0.606, 0.820), respectively. Although these two glycopeptides were significantly different between cirrhosis and HCC, they did not yield a better AUC than AFP alone (Figure S5a,b, red lines). The four glycopeptides involving glycosite N241 (Figure S5c–e, red lines) included one bi-antennary glycopeptide N241_A2G2F1S2, one tri-antennary glycopeptide

Table 3. The Best 2-Marker and 3-Marker Panels in Differentiating all HCCs and Early-Stage HCCs, Respectively^a

cirrhosis (<i>n</i> = 46) vs all HCC (<i>n</i> = 49)					
	best model	AUC	95% CI	sensitivity at 90% specificity	<i>P</i>
	AFP	0.79	(0.697, 0.872)	52.30%	NA
2-marker	AFP + N241_A4G4F2S4	0.898	(0.835, 0.951)	63.30%	0.0481
3-marker	AFP + N241_A2G2F1S2 + N241_A4G4F2S4	0.928	(0.877, 0.970)	65.30%	0.0083
cirrhosis (<i>n</i> = 46) vs early HCC (<i>n</i> = 32)					
	best model	AUC	95% CI	sensitivity at 90% specificity	<i>P</i>
	AFP	0.715	(0.592, 0.827)	39.50%	NA
2-marker	AFP + N241_A4G4F2S4	0.845	(0.757, 0.919)	50.00%	0.0691
3-marker	AFP + age + N241_A2G2F1S2	0.902	(0.829, 0.961)	71.90%	0.0048

^a*p*-Values were based on the bootstrapping method of 1000 bootstrapping samples.

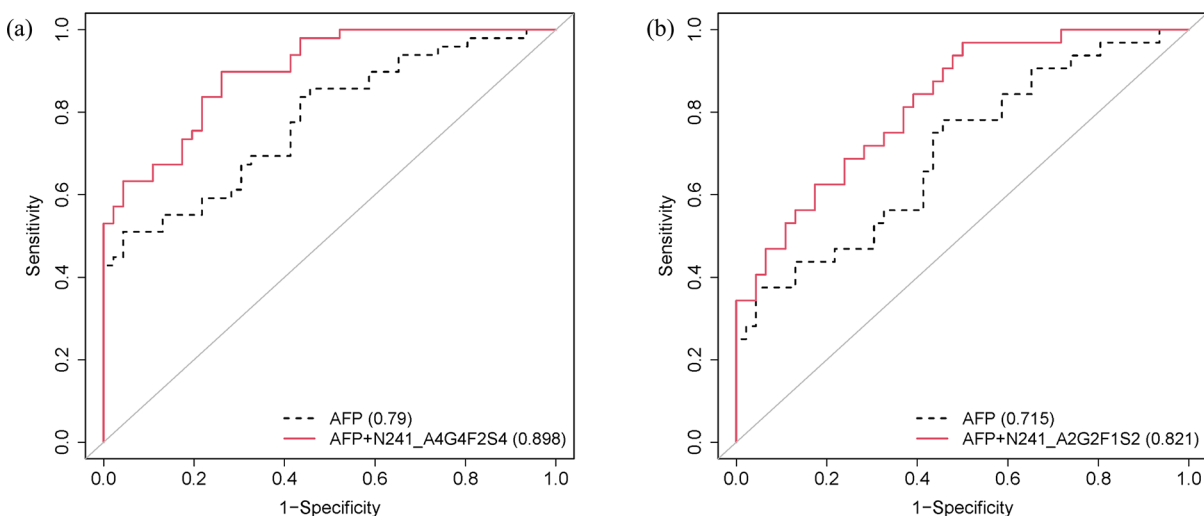


Figure 6. ROC curves of the best 2-marker panel to differentiate all HCCs (a), and early HCCs (b) from cirrhosis patients (black dashed line, AFP only; red solid line, combined Hp *N*-glycopeptide and AFP).

N241_A3G3F1S3, and two tetra-antennary glycopeptides N241_A4G4F1S3 and N241_A4G4F2S4. N241_A3G3F1S3 and N241_A4G4F2S4 had similar estimated AUC as AFP, 0.796 (95% CI: 0.693, 0.883) and 0.793 (95% CI: 0.700, 0.874), respectively.

When comparing early-stage HCCs to cirrhosis, AFP had an estimated AUC of 0.715 (95% CI: 0.592, 0.827). It had a sensitivity of 39.5 at 90% specificity. Like the results of all HCCs together, the results from glycopeptides involving site N184 did not perform better than that of AFP alone (Figure S6a,b, red solid lines). However, the glycopeptides N241_A2G2F1S2 (Figure S6e, red solid lines), N241_A3G3F1S3 (Figure S6c, red solid lines), and N241_A4G4F2S4 (Figure S6f, red solid lines) showed slightly better AUC, and their AUCs were 0.732 (95% CI: 0.617, 0.832), 0.729 (95% CI: 0.611, 0.836), and 0.757 (95% CI: 0.643, 0.861), respectively.

Diagnostic Performance of Combinatorial Analysis of Hp *N*-Glycopeptide Markers with AFP. In order to improve the discrimination performance of AFP, we sought the best combination panels. Considering six candidate glycopeptide markers, as well as age and gender, using AFP as the anchor marker, we built the 2-marker and 3-marker panels. The marker panels with the highest AUC were selected as the best panel for future validation. Table 3 summarizes the results of the best 2- and 3-marker panels. The *p*-values for

comparing each selected marker panel with the panel using AFP alone were calculated based on the bootstrapping method.

All the 2-marker combination models showed AUCs greater than 0.841 in distinguishing all HCC samples from cirrhosis (Table S2) and better than the AUC of 0.790 using AFP alone. N241_A4G4F2S4 combined with AFP had the best estimated AUC in all 2-marker combinations with an estimated AUC of 0.898 (95% CI: 0.835, 0.951), which was significantly better than AFP alone (*P* = 0.0481) (Figure 6a). This best 2-marker panel had a sensitivity of 63.3% at 90% specificity, whereas AFP alone had a sensitivity of 52.3%. When using 3-fold cross validation, it had an AUC of 0.904 (95% CI: 0.844, 0.960). The other three glycopeptides on site 241, involving N241_A2G2S1F2, N241_A3G3F1S3, and N241_A4G4F1S3, achieved AUC values of 0.870 (Figure S5e), 0.869 (Figure S5c), and 0.841 (Figure S5d), respectively. The sensitivities for each at 90% specificity were 59.2, 57.1, and 61.2%. At site N184, the AUC for the combination for glycopeptide N184_A3G3F1S3 + AFP was estimated to be 0.843 (95% CI: 0.763, 0.917) (Figure S5a, green solid line). Also, the panel of N184_A2G2S2 + AFP had an AUC of 0.869 (95% CI: 0.795, 0.931). Notably, this glycopeptide's expression is decreased in distinguishing between HCCs to cirrhosis, where there is no Sialyl Lewis epitope.

In the comparison of early-stage HCC vs cirrhosis, the panel of AFP + N241_A4G4F2S4 had the best estimated AUC of 0.845 (95% CI: 0.757, 0.919), which was marginally

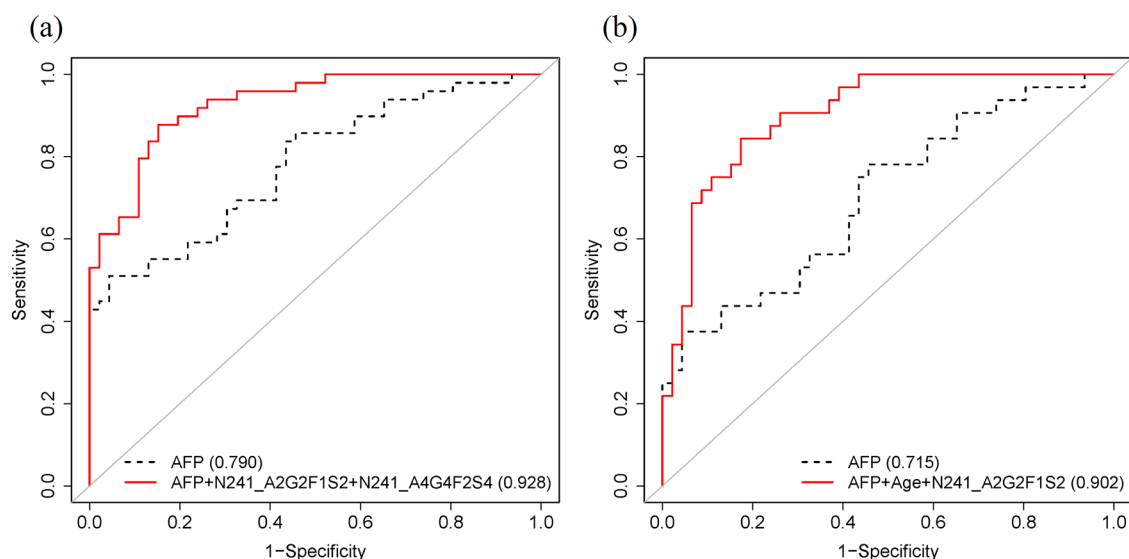


Figure 7. ROC curves of the best 3-marker panel to differentiate all HCCs (a) and early HCCs (b) from cirrhosis patients (black dashed line, AFP only; red solid line, combined Hp *N*-glycopeptide and AFP).

significantly better than the AUC of 0.715 (95% CI: 0.592, 0.827) when using AFP alone ($P = 0.0691$) (Figure 6b). It had a sensitivity of 50.0% at 90% specificity, whereas AFP alone had a sensitivity of 39.5%. Its AUC was estimated to be 0.823 (95% CI: 0.750, 0.923) in 3-fold cross validation.

Similar to the results from all HCCs, in early-stage HCC, the AUC values of the other three glycopeptides N241_A2G2F1S2, N241_A3G3F1S3, and N241_A4G4F1S3 were larger than 0.762, and they had better sensitivity at 90% specificity than AFP alone in distinguishing early-stage HCCs from cirrhosis (Table S2 and Figure S6c–f). At site N184, the AUC value of N184_A2G2S2 combined with AFP was 0.806, and the AUC of N184_A3G3F1S3 + AFP was 0.777 (Figure S6a,b). It is notable that the glycopeptide N241_A4G4F2S4 combined with AFP provided the best AUC values among these glycopeptides either in distinguishing all HCCs or early-stage HCC from cirrhosis.

Since both age and gender showed significant differences between cirrhosis and HCC samples, we also tested the performance of the 2-marker panels of AFP + age and AFP + gender. When differentiating all HCC, the panels of AFP + age and AFP + gender had the estimated AUC being 0.846 (95% CI: 0.760, 0.916) and 0.811 (95% CI: 0.714, 0.890), respectively. When differentiating early HCC, the panels of AFP + age and AFP + gender had the estimated AUC of 0.832 (95% CI: 0.734, 0.906) and 0.761 (95% CI: 0.650, 0.858), respectively. None of them had significant improvement compared to AFP alone.

Diagnostic Performance of Combinatorial Analysis Using 3-Marker Panels. When considering 3-marker panels and using AFP as the anchor marker, the best panel was selected based on the estimated AUC. The performance of the best panel is summarized in Table 3, and Figure 7 shows the ROCs.

In the results for all HCC vs cirrhosis, the combination of AFP + N241_A2G2F1S2 + N241_A4G4F2S4 performed the best with the AUC estimated to be 0.928 (95% CI: 0.877, 0.970), with 65.3% sensitivity at 90% specificity. It was statistically better than the panel using AFP alone ($P = 0.0083$). When using 3-fold cross validation, it had an AUC of

0.923 (95% CI: 0.874, 0.975). In the comparison of early-stage HCCs vs cirrhosis, the combination of AFP + age + N241_A2G2F1S2 performed the best with an achieved AUC value of 0.902 (95% CI: 0.829, 0.961), with 71.9% sensitivity at 90% specificity. It was statistically better than the panel using AFP alone ($P = 0.0048$). When using 3-fold cross validation, it had an AUC of 0.885 (95% CI: 0.861, 0.967).

CONCLUSIONS

In this study, we demonstrated that six fucosylated glycopeptides from serum Hp based on subtle glycan structural changes could differentiate HCC from cirrhosis in patients with NASH using LC-stepped HCD-PRM-MS/MS ($P < 0.05$). These six glycopeptides involved two glycopeptides at site N184 and four glycopeptides at site N241. At site N184, the expression of the glycopeptide N184_A2G2S2 without Sialyl Lewis epitopes decreased in distinguishing all HCCs from cirrhosis. Another glycopeptide involving site N184, N184_A3G3F1S3, and the four glycopeptides bearing N241 glycans with Sialyl Lewis epitopes were expressed differentially during disease progression.

The ROC curves of all these glycopeptides when combined with AFP performed better than AFP alone. Of these fucosylated glycopeptides, a tetra-antennary N241_A4G4F2S4 provided the best performance with an AUC value of 0.898 (95% CI: 0.835, 0.951, sensitivity: 63.3%, specificity: 90%) for the comparison of all HCCs versus cirrhosis. When considering 3-marker panels, the AUC value of the combination of AFP + N241_A2G2F1S2 + N241_A4G4F2S4 performed the best in all HCCs. These results demonstrated that the bifucosylated tetra-antennary glycopeptides N241_A4G4F2S4, which bear the Sialyl Lewis (SLe) epitope, may potentially play a role in distinguishing HCC from cirrhosis. The bifucosylated tetra-antennary glycopeptide at site N241 contains both a core-fucosylation and an outer-arm fucosylation. These markers are promising for early detection of HCC but still require validation in a larger sample set for further evaluation.

■ ASSOCIATED CONTENT

SI Supporting Information

The Supporting Information is available free of charge at <https://pubs.acs.org/doi/10.1021/acsomega.2c02600>.

Haptoglobin standard curve, representative MS/MS spectra of N-glycopeptides involving sites N184 and N241 as well as their ROC curves, and precursor ions for PRM (PDF)

■ AUTHOR INFORMATION

Corresponding Authors

Jianhui Zhu – Department of Surgery, University of Michigan Medical Center, Ann Arbor, Michigan 48109, United States; orcid.org/0000-0002-0051-7777; Phone: 734-615-2567; Email: jianhuiz@umich.edu; Fax: 734-615-2088

David M. Lubman – Department of Surgery, University of Michigan Medical Center, Ann Arbor, Michigan 48109, United States; orcid.org/0000-0001-7731-0232; Phone: 734-647-8834; Email: dmlubman@umich.edu; Fax: 734-615-2088

Authors

Yu Lin – Department of Surgery, University of Michigan Medical Center, Ann Arbor, Michigan 48109, United States

Jie Zhang – Department of Surgery, University of Michigan Medical Center, Ann Arbor, Michigan 48109, United States; orcid.org/0000-0002-1395-4853

Jianliang Dai – Department of Biostatistics, University of Texas MD Anderson Cancer Center, Houston, Texas 77030, United States

Suyu Liu – Department of Biostatistics, University of Texas MD Anderson Cancer Center, Houston, Texas 77030, United States

Ana Arroyo – Department of Internal Medicine, University of Texas Southwestern Medical Center, Dallas, Texas 75390, United States

Marissa Rose – Department of Internal Medicine, University of Texas Southwestern Medical Center, Dallas, Texas 75390, United States

Amit G. Singal – Department of Internal Medicine, University of Texas Southwestern Medical Center, Dallas, Texas 75390, United States

Neelhar D. Parikh – Division of Gastroenterology and Hepatology, University of Michigan Medical Center, Ann Arbor, Michigan 48109, United States

Complete contact information is available at:

<https://pubs.acs.org/doi/10.1021/acsomega.2c02600>

Notes

The authors declare no competing financial interest.

■ ACKNOWLEDGMENTS

We acknowledge the support of this work from the National Cancer Institute under grants 1R01 CA160254 (DML) and U01 CA225753 (DML). The Orbitrap instrument was purchased under an NIH shared instrumentation grant S10OD021619. A.G.S. acknowledges the support from the National Cancer Institute under grant U01 CA230694 (AGS). D.M.L. acknowledges support under the Maud T. Lane Professorship. We also acknowledge the support of this work from Protein Metrics Inc. for the use of the Byonic/Byologic software.

■ REFERENCES

- (1) Singal, A. G.; El-Serag, H. B. Hepatocellular carcinoma from epidemiology to prevention: translating knowledge into practice. *Clin. Gastroenterol. Hepatol.* **2015**, *13*, 2140–2151.
- (2) Kulik, L.; El-Serag, H. B. Epidemiology and management of hepatocellular carcinoma. *Gastroenterology* **2019**, *156*, 477–491.e1.
- (3) Sanduzzi-Zamparelli, M.; Díaz-Gonzalez, Á.; Reig, M. New systemic treatments in advanced hepatocellular carcinoma. *Liver Transplant.* **2019**, *25*, 311–322.
- (4) Singal, A. G.; Pillai, A.; Tiro, J. Early detection, curative treatment, and survival rates for hepatocellular carcinoma surveillance in patients with cirrhosis: a meta-analysis. *PLoS Med.* **2014**, *11*, No. e1001624.
- (5) Schoenberger, H.; Chong, N.; Fetzer, D. T.; Rich, N. E.; Yokoo, T.; Khatri, G.; Olivares, J.; Parikh, N. D.; Yopp, A. C.; Marrero, J. A.; Singal, A. G. Dynamic changes in ultrasound quality for hepatocellular carcinoma screening in patients with cirrhosis. *Clin. Gastroenterol. Hepatol.* **2022**, 1561.
- (6) Tzartzeva, K.; Obi, J.; Rich, N. E.; Parikh, N. D.; Marrero, J. A.; Yopp, A.; Waljee, A. K.; Singal, A. G. Surveillance imaging and alpha fetoprotein for early detection of hepatocellular carcinoma in patients with cirrhosis: a meta-analysis. *Gastroenterology* **2018**, *154*, 1706–1718.e1.
- (7) Lin, Y.; Zhu, J.; Pan, L.; Zhang, J.; Tan, Z.; Olivares, J.; Singal, A. G.; Parikh, N. D.; Lubman, D. M. A panel of glycopeptides as candidate biomarkers for early diagnosis of nash hepatocellular carcinoma using a stepped hcd method and prm evaluation. *J. Proteome Res.* **2021**, *20*, 3278–3289.
- (8) Singal, A. G.; Hoshida, Y.; Pinato, D. J.; Marrero, J.; Nault, J. C.; Paradis, V.; Tayob, N.; Sherman, M.; Lim, Y. S.; Feng, Z.; Lok, A. S.; Rinaudo, J. A.; Srivastava, S.; Llovet, J. M.; Villanueva, A. International liver cancer association (ilca) white paper on biomarker development for hepatocellular carcinoma. *Gastroenterology* **2021**, *160*, 2572–2584.
- (9) Parikh, N. D.; Mehta, A. S.; Singal, A. G.; Block, T.; Marrero, J. A.; Lok, A. S. Biomarkers for the early detection of hepatocellular carcinoma. *Cancer Epidemiol. Biomark. Prev.* **2020**, *29*, 2495–2503.
- (10) Lin, Y.; Zhang, J.; Arroyo, A.; Singal, A. G.; Parikh, N. D.; Lubman, D. M. A fucosylated glycopeptide as a candidate biomarker for early diagnosis of NASH hepatocellular carcinoma using a stepped HCD method and PRM evaluation. *Front. Oncol.* **2022**, 12.
- (11) Liang, Y.; Fu, B.; Zhang, Y.; Lu, H. Progress of proteomics driven precision medicine—from a glycosylation view. *Rapid Commun. Mass Spectrom.* **2022**, DOI: 10.1002/rcm.9288
- (12) Gopal, P.; Yopp, A. C.; Waljee, A. K.; Chiang, J.; Nehra, M.; Kandunoori, P.; Singal, A. G. Factors that affect accuracy of alpha-fetoprotein test in detection of hepatocellular carcinoma in patients with cirrhosis. *Clin. Gastroenterol. Hepatol.* **2014**, *12*, 870–877.
- (13) Li, D.; Mallory, T.; Satomura, S. AFP-L3: a new generation of tumor marker for hepatocellular carcinoma. *Clin. Chim. Acta* **2001**, *313*, 15–19.
- (14) Mehta, A.; Block, T. M. Fucosylated glycoproteins as markers of liver disease. *Dis. Markers* **2008**, *25*, 259–265.
- (15) Ohtsubo, K.; Marth, J. D. Glycosylation in cellular mechanisms of health and disease. *Cell* **2006**, *126*, 855–867.
- (16) Sun, S. S.; Zhang, H. Large-scale measurement of absolute protein glycosylation stoichiometry. *Anal. Chem.* **2015**, *87*, 6479–6482.
- (17) Zhu, J.; Warner, E.; Parikh, N. D.; Lubman, D. M. Glycoproteomic markers of hepatocellular carcinoma—mass spectrometry based approaches. *Mass Spectrom. Rev.* **2019**, *38*, 265–290.
- (18) Yin, H.; Lin, Z.; Nie, S.; Wu, J.; Tan, Z.; Zhu, J.; Dai, J.; Feng, Z.; Marrero, J.; Lubman, D. M. Mass-selected site-specific core-fucosylation in ceruloplasmin in alcohol-related hepatocellular carcinoma. *J. Proteome Res.* **2014**, *13*, 2887–2896.
- (19) Qin, H.; Dong, X.; Mao, J.; Chen, Y.; Dong, M.; Wang, L.; Guo, Z.; Liang, X.; Ye, M. Highly efficient analysis of glycoprotein sialylation in human serum by simultaneous quantification of glycosites and site-specific glycoforms. *J. Proteome Res.* **2019**, *18*, 3439–3446.

- (20) Yin, H.; Zhu, J.; Wang, M.; Yao, Z.-P.; Lubman, D. M. Quantitative analysis of α -1-antitrypsin glycosylation isoforms in HCC patients using LC-HCD-PRM-MS. *Anal. Chem.* **2020**, *92*, 8201–8208.
- (21) Fagoonee, S.; Gburek, J.; Hirsch, E.; Marro, S.; Moestrup, S. K.; Laurberg, J. M.; Christensen, E. L.; Silengo, L.; Altruda, F.; Tolosano, E. Plasma protein haptoglobin modulates renal iron loading. *Am. J. Pathol.* **2005**, *166*, 973–983.
- (22) Zhu, J.; Huang, J.; Zhang, J.; Chen, Z.; Lin, Y.; Grigorean, G.; Li, L.; Liu, S.; Singal, A. G.; Parikh, N. D.; Lubman, D. M. Glycopeptide biomarkers in serum haptoglobin for hepatocellular carcinoma detection in patients with non-alcoholic steatohepatitis. *J. Proteome Res.* **2020**, *19*, 3452–3466.
- (23) Zhu, J.; Chen, Z.; Zhang, J.; An, M.; Wu, J.; Yu, Q.; Skilton, S. J.; Bern, M.; Sen, K. I.; Li, L.; Lubman, D. M. Differential quantitative determination of site-specific intact N-glycopeptides in serum haptoglobin between hepatocellular carcinoma and cirrhosis using LC-ETHcD-MS/MS. *J. Proteome Res.* **2019**, *18*, 359–371.
- (24) Sanda, M.; Pompach, P.; Brnakova, Z.; Wu, J.; Makambi, K.; Goldman, R. Quantitative liquid chromatography-mass spectrometry-multiple reaction monitoring (LC-MS-MRM) analysis of site-specific glycoforms of haptoglobin in liver disease. *Mol. Cell. Proteomics* **2013**, *12*, 1294–1305.
- (25) Pompach, P.; Brnakova, Z.; Sanda, M.; Wu, J.; Edwards, N.; Goldman, R. Site-specific glycoforms of haptoglobin in liver cirrhosis and hepatocellular carcinoma. *Mol. Cell. Proteomics* **2013**, *12*, 1281–1293.
- (26) Ramachandran, P.; Xu, G.; Huang, H. H.; Rice, R.; Zhou, B.; Lindpaintner, K.; Serie, D. Serum glycoprotein markers in non-alcoholic steatohepatitis and hepatocellular carcinoma. *J. Proteome Res.* **2022**, 1083.
- (27) Suttapitugsakul, S.; Sun, F.; Wu, R. Recent advances in glycoproteomic analysis by mass spectrometry. *Anal. Chem.* **2020**, *92*, 267–291.
- (28) Yu, Q.; Wang, B.; Chen, Z.; Urabe, G.; Glover, M. S.; Shi, X.; Guo, L. W.; Kent, K. C.; Li, L. Electron-transfer/higher-energy collision dissociation (ETHcD)-enabled intact glycopeptide/glycopeptide characterization. *J. Am. Soc. Mass Spectrom.* **2017**, *28*, 1751–1764.
- (29) Patwa, T.; Li, C.; Simeone, D. M.; Lubman, D. M. Glycoprotein analysis using protein microarrays and mass spectrometry. *Mass Spectrom. Rev.* **2010**, *29*, 830–844.
- (30) Ang, I. L.; Poon, T. C. W.; Lai, P. B. S.; Chan, A. T. C.; Ngai, S.-M.; Hui, A. Y.; Johnson, P. J.; Sung, J. J. Y. Study of serum haptoglobin and its glycoforms in the diagnosis of hepatocellular carcinoma: a glycoproteomic approach. *J. Proteome Res.* **2006**, *5*, 2691–2700.
- (31) Zhang, S.; Shu, H.; Luo, K.; Kang, X.; Zhang, Y.; Lu, H.; Liu, Y. N-linked glycan changes of serum haptoglobin β chain in liver disease patients. *Mol. Biosyst.* **2011**, *7*, 1621–1628.
- (32) Zhu, J.; Lin, Z.; Wu, J.; Yin, H.; Dai, J.; Feng, Z.; Marrero, J.; Lubman, D. M. Analysis of serum haptoglobin fucosylation in hepatocellular carcinoma and liver cirrhosis of different etiologies. *J. Proteome Res.* **2014**, *13*, 2986–2997.
- (33) Rich, N. E.; Murphy, C. C.; Yopp, A. C.; Tiro, J.; Marrero, J. A.; Singal, A. G. Sex disparities in presentation and prognosis of 1110 patients with hepatocellular carcinoma. *Aliment. Pharmacol. Ther.* **2020**, *52*, 701–709.
- (34) Rich, N. E.; Hester, C.; Odewole, M.; Murphy, C. C.; Parikh, N. D.; Marrero, J. A.; Yopp, A. C.; Singal, A. G. Racial and ethnic differences in presentation and outcomes of hepatocellular carcinoma. *Clin. Gastroenterol. Hepatol.* **2019**, *17*, 551–559.e1.
- (35) Hester, C. A.; Rich, N. E.; Singal, A. G.; Yopp, A. C. Comparative analysis of nonalcoholic steatohepatitis- versus viral hepatitis- and alcohol-related liver disease-related hepatocellular carcinoma. *J. Natl. Compr. Cancer Network* **2019**, *17*, 322–329.
- (36) van der Pol, C. B.; Lim, C. S.; Sirlin, C. B.; McGrath, T. A.; Salameh, J. P.; Bashir, M. R.; Tang, A.; Singal, A. G.; Costa, A. F.; Fowler, K.; McInnes, M. D. F. Accuracy of the liver imaging reporting and data system in computed tomography and magnetic resonance image analysis of hepatocellular carcinoma or overall malignancy-a systematic review. *Gastroenterology* **2019**, *156*, 976–986.
- (37) Marrero, J. A.; Kulik, L. M.; Sirlin, C. B.; Zhu, A. X.; Finn, R. S.; Abecassis, M. M.; Roberts, L. R.; Heimbach, J. K. Diagnosis, staging, and management of hepatocellular carcinoma: 2018 practice guidance by the american association for the study of liver diseases. *Hepatology* **2018**, *68*, 723–750.
- (38) Huang, Y.; Zhou, S.; Zhu, J.; Lubman, D. M.; Mechref, Y. LC-MS/MS isomeric profiling of permethylated N-glycans derived from serum haptoglobin of hepatocellular carcinoma (HCC) and cirrhotic patients. *Electrophoresis* **2017**, *38*, 2160–2167.
- (39) Zhu, J.; Wu, J.; Yin, H.; Marrero, J.; Lubman, D. M. Mass spectrometric N-glycan analysis of haptoglobin from patient serum samples using a 96-well plate format. *J. Proteome Res.* **2015**, *14*, 4932–4939.
- (40) Chandler, K. B.; Pompach, P.; Goldman, R.; Edwards, N. Exploring site-specific N-glycosylation microheterogeneity of haptoglobin Using glycopeptide CID tandem mass spectra and glycan database search. *J. Proteome Res.* **2013**, *12*, 3652–3666.
- (41) Peterson, A. C.; Russell, J. D.; Bailey, D. J.; Westphall, M. S.; Coon, J. J. Parallel reaction monitoring for high resolution and high mass accuracy quantitative, targeted proteomics. *Mol. Cell. Proteomics* **2012**, *11*, 1475–1488.
- (42) Kamada, Y.; Ono, M.; Hyogo, H.; Fujii, H.; Sumida, Y.; Mori, K.; Tanaka, S.; Yamada, M.; Akita, M.; Mizutani, K.; Fujii, H.; Yamamoto, A.; Takamatsu, S.; Yoshida, Y.; Itoh, Y.; Kawada, N.; Chayama, K.; Saibara, T.; Takehara, T.; Miyoshi, E. A novel noninvasive diagnostic method for nonalcoholic steatohepatitis using two glyco-biomarkers. *Hepatology* **2015**, *62*, 1433–1443.
- (43) Rauniyar, N. Parallel reaction monitoring: a targeted experiment performed using high resolution and high mass accuracy mass spectrometry. *Int. J. Mol. Sci.* **2015**, *16*, 28566–28581.
- (44) van Bentum, M.; Selbach, M. An introduction to advanced targeted acquisition methods. *Mol. Cell. Proteomics* **2021**, *20*, No. 100165.
- (45) Panigrahi, A.; Benicky, J.; Wei, R.; Ahn, J.; Goldman, R.; Sanda, M. A rapid LC-MS/MS-PRM assay for serologic quantification of sialylated O-HPX glycoforms in patients with liver fibrosis. *Molecules* **2022**, *27*, 2213.
- (46) Gutierrez Reyes, C. D.; Huang, Y.; Atashi, M.; Zhang, J.; Zhu, J.; Liu, S.; Parikh, N. D.; Singal, A. G.; Dai, J.; Lubman, D. M.; Mechref, Y. PRM-MS quantitative analysis of isomeric N-glycopeptides derived from human serum haptoglobin of patients with cirrhosis and hepatocellular carcinoma. *Metabolites* **2021**, *11*, 563.
- (47) Zhang, Y.; Zhu, J.; Yin, H.; Marrero, J.; Zhang, X.-X.; Lubman, D. M. ESI-LC-MS method for haptoglobin fucosylation analysis in hepatocellular carcinoma and liver cirrhosis. *J. Proteome Res.* **2015**, *14*, 5388–5395.
- (48) Oh, M. J.; Lee, S. H.; Kim, U.; An, H. J. In-depth investigation of altered glycosylation in human haptoglobin associated cancer by mass spectrometry. *Mass Spectrom. Rev.* **2021**, DOI: 10.1002/mas.21707
- (49) Ferens-Sieczkowska, M.; Kratz, E. M.; Kossowska, B.; Passowicz-Muszyńska, E.; Jankowska, R. Comparison of haptoglobin and α ₁-acid glycoprotein glycosylation in the sera of small cell and non-small cell lung cancer patients. *Postepy Hig. Med. Dosw.* **2013**, *67*, 828–836.
- (50) Tang, H.; Singh, S.; Partyka, K.; Kletter, D.; Hsueh, P.; Yadav, J.; Ensink, E.; Bern, M.; Hostetter, G.; Hartman, D.; Huang, Y.; Brand, R. E.; Haab, B. B. Glycan motif profiling reveals plasma sialyl-lewis X elevations in pancreatic cancers that are negative for sialyl-lewis A*. *Mol. Cell. Proteomics* **2015**, *14*, 1323–1333.
- (51) Saldova, R.; Royle, L.; Radcliffe, C. M.; Abd Hamid, U. M.; Evans, R.; Arnold, J. N.; Banks, R. E.; Hutson, R.; Harvey, D. J.; Antobus, R.; Petrescu, S. M.; Dwek, R. A.; Rudd, P. M. Ovarian cancer is associated with changes in glycosylation in both acute-phase proteins and IgG. *Glycobiology* **2007**, *17*, 1344–1356.